Available online at www.sciencedirect.com
ScienceDirect
Composites: Part B 38 (2007) 772–780
composites
Part B: engineering
www.elsevier.com/locate/compositesb

Shear creep of epoxy at the concrete–FRP interfaces

Kyoung-Kyu Choi, Pania Meshgin, Mahmoud M. Reda Taha *

Department of Civil Engineering, University of New Mexico, MSC01 1070, 1 University of New Mexico, NM 87131-0001, USA

Received 20 May 2006; accepted 9 October 2006
Available online 23 January 2007

Abstract

This paper presents the results of experimental and analytical investigations of the long-term behavior of the epoxy used at the concrete–FRP interfaces. Double shear long-term test was performed on specimens composed of concrete blocks bonded to FRP sheets using epoxy. Three test replicates were examined under sustained shear stress for up to six month time period with two primary parameters: the shear stress level and the epoxy thickness. The investigation showed that shear stress level might have significant effect on the long-term behavior of epoxy at the concrete–FRP interfaces. Based on the experimental results, creep characteristics of epoxy in the concrete–FRP interfaces were evaluated. Finite element analysis was performed incorporating these creep characteristics to investigate the long-term deformations and stress redistributions in the test specimens. It was recognized that creep of epoxy might result in stress-redistribution at the concrete–FRP interfaces.

Keywords: A. Carbon fibre; B. Creep; C. Finite element analysis; D. Mechanical testing

1. Introduction

The need for rehabilitation and strengthening of existing reinforced concrete structures is increasing with the continued aging of infrastructure. Moreover, strengthening may be needed to upgrade the structural capacity to accommodate increasing loads or modified uses. Fiber reinforced polymer (FRP) composite materials have been considered an efficient alternative for rehabilitation and strengthening due to their various advantages [1,2]. For instance, the external installation of FRP strips can provide the required additional strength for an existing bridge deck slab to accommodate additional live loads. Furthermore, since FRP composites are lighter compared with steel reinforcement, using FRP does not increase significantly dead load of the structure. Prestressed FRP has also been used for their relatively low prestress losses as a result of their relatively low elastic modulus [1] and significantly low stress relaxation compared with steel strands [3].

In reinforced concrete structures strengthened with externally bonded FRP, it is well established that the key factor affecting the performance is the bond between concrete and FRP. Many experimental and analytical studies have been performed to investigate the bond behavior of the concrete–FRP interfaces [4–7]. These investigations established that the bond-slip relationship between concrete and FRP is capable of explaining the debonding failure mechanism [8] and ultimate bond strength. Niedermeier [9], Hiroyuki and Wu [10] and Teng et al. [11] recognized that the bond strength does not increase with increasing the FRP/concrete bond length. These findings lead to the concept of effective bond length adopted by many design guidelines [12,13]. Moreover, researchers including Hiroyuki and Wu [10] and Teng et al. [11] developed various bond strength models as stress-based models [14], fracture mechanics models [9] and empirical models [10].

However, almost all of these investigations were based on instantaneous shear tests using single-, double-shear test setups, and beam test setup [11]. The effect of the adhesive characteristics on the bond behavior between concrete and FRP has not been satisfactorily investigated. According to

* Corresponding author. Tel.: +1 505 277 1258; fax: +1 505 277 1988.
E-mail address: mrtaha@unm.edu (M.M. Reda Taha).

1359-8368/$ - see front matter © 2007 Elsevier Ltd. All rights reserved.
doi:10.1016/j.compositesb.2006.10.003

Chen and Teng [14], the concrete–adhesive interfaces are susceptible to micro cracking, which initiates the debonding failure of concrete–FRP composites. Furthermore, since concrete–epoxy–FRP composite is composed of three different materials showing different long-term material properties, the long-term behavior including creep deformation and stress redistribution in this composite represents a complex process that needs further investigation.

In the present study, we performed experimental investigation examining the long-term behavior of epoxy at the concrete–FRP interfaces using double shear test setup. The test specimens composed of concrete blocks bonded to FRP sheets using epoxy. The specimens were examined under sustained shear stress (at the service load level) for up to six month time period. In addition, finite element analysis was performed to investigate the long-term deformation and stress redistribution in the concrete–FRP interfaces.

2. Methods

2.1. Experimental methods

In this article, the experimental study includes examining shear creep of epoxy at the concrete–FRP interfaces. Double shear test experiments were carried out using concrete blocks bonded to FRP sheets using epoxy as shown in Fig. 1. It is noted that the steel bars shown in Fig. 1 are not bonded to concrete. Other researchers (e.g. [15]) suggested that the simple shear experiments including single- and double- shear test setups can properly simulate the debonding mechanism at the concrete–FRP interfaces.

Specific concrete mix was used to produce the concrete blocks used in the experiments. The concrete mix included sand, 1750 kg/m^3; Type I Portland cement, 500 kg/m^3; and water 282 kg/m^3. The choice of the concrete mix was based on achieving a specific tensile strength to avoid failure of the shear experiments in the concrete interface. Concrete was cast according to typical mixing methods using a standard concrete mixer. The mean compressive strength at 28 day of age for ($50 \times 50 \times 50$ mm) cubes was 38 MPa after 7 day curing in a water bath at fixed temperature of 20 °C.

Carbon fiber reinforced polymer (CFRP) sheets were used as the strengthening material. The tensile strength and elastic modulus of the CFRP sheets, as reported by the manufacturer's datasheet, are provided in Table 1. Ordinary epoxy, usually used in practical FRP applications, was selected as the structural adhesive. The epoxy was made by mixing the resin and the hardener with a ratio of 1:1. The ingredients and the mechanical properties of the epoxy as reported by its manufacturer are presented in Table 1. The epoxy was mixed according to the procedure recommended by the manufacturer. Before mixing, the surface of concrete was made clean, dry and free of oil, and the resin and the hardener were mixed thoroughly until both blend into uniform color. Moreover, the epoxy was applied to concrete within 5 min after mixing. In this experimental study, epoxy was cured by allowing it to dry in the laboratory environment (50% relative humidity and 20 °C). Two curing periods were considered: 1 day and 7 day. According to the manufacturer's datasheet, 90% of the mechanical properties of the epoxy shall be developed after 1 day of such curing. It is important to note that typically two types of resins (a saturant resin and an adhesive resin)

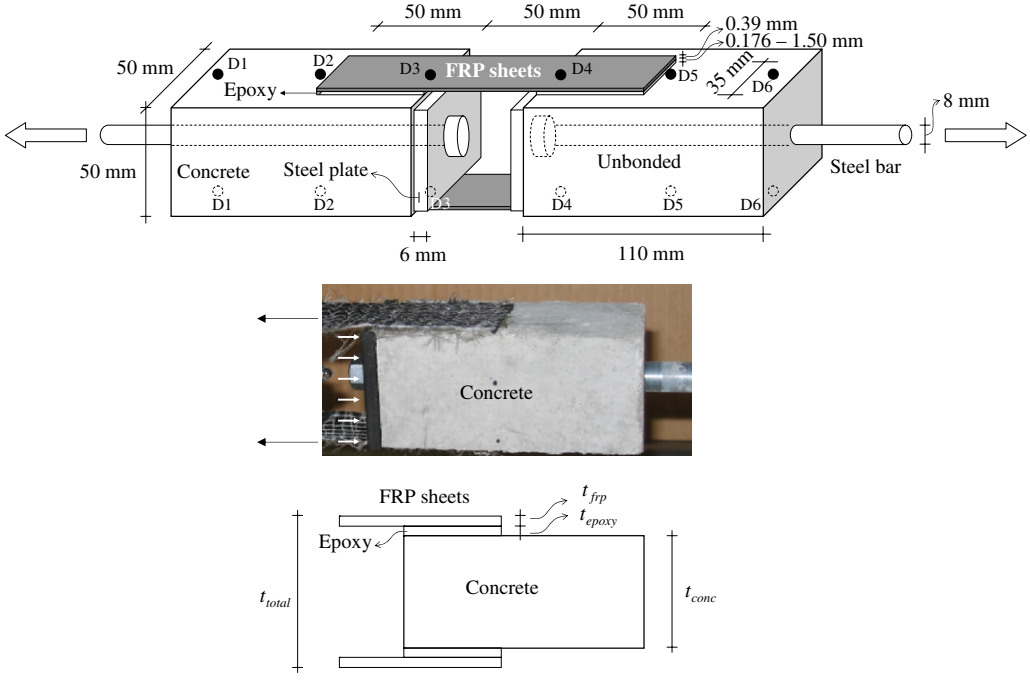

Fig. 1. Double-shear test specimens composed of concrete blocks, epoxy and FRP sheets.

Table 1
Materials properties of CFRP and epoxy

CFRP[a]	
Tensile strength (MPa)	3860
Elastic modulus (GPa)	242
Epoxy[b]	
Ingredient of resin (%)	Epichlorohydrin (60–100) Silica (1–5)
Ingredient of hardener (%)	Polymercaptan (60–100) Phenol (5–10) Silica (5–10) Ethylene glycol (1–5)
Specific gravity	1.16
Shear strength after 1 h curing (MPa)	10.3
Shear strength after 24 h curing (MPa)	13.7

[a] Reported by CFRP manufacturer.
[b] Reported by epoxy manufacturer.

are used in the wet lay-up process [12,13] for the application of FRP sheets to concrete. However, given the objective of this study to investigate creep behavior of the epoxy adhesive at the interface, the saturant resin was not applied intentionally. This is because of the fact that, saturating the CFRP sheets in the saturant resin would add additional source of creep at the interface. Separating the two creep components; creep from the saturant and creep from the epoxy adhesive, might not be possible and would complicate the analysis considerably. Therefore, the use of the saturant resin was avoided here.

Specimens for the double-shear test were composed of two concrete blocks, epoxy, and two FRP sheets (Fig. 1). The two concrete blocks were connected by FRP sheets in top and bottom faces, and the concrete and FRP sheets were bonded using epoxy. The dimensions of the concrete blocks were $50 \times 50 \times 110$ mm while the FRP sheets were 35 wide $\times$ 0.39 thickness $\times$ 150 long mm, as shown in Fig. 1. The concrete blocks used in the experiment were cured for 28 days of age. The FRP and epoxy was applied to concrete. After FRP application, the specimens were cured in the dry laboratory environment as explained above for 1 day or 7 day time period.

The parameters examined in the experiments were the shear stress level represented by the shear stress to ultimate shear strength ratio, the thickness of the epoxy layer and the curing time of epoxy. Combinations of these parameters lead to nine testing specimens. The specimens were subjected to sustained shear stress for 6 month time period. For space limitations we report the results and analysis of three specimens only considering the effect of shear stress level and epoxy layer thickness. Complete details and experimental results of the nine specimens can be found elsewhere [16].

Here, two specific shear stress levels of 0.09 MPa and 0.17 MPa, were used. According to the results of ultimate shear strength tests performed on specimens made of similar concrete blocks, epoxy and FRP sheets, the mean ultimate shear strength of the double shear test specimens was 0.56 MPa [16]. Therefore, the shear stress levels used in this study corresponds to 15% and 31% of the ultimate shear strength, respectively, representing two different service stress levels. The thickness of epoxy used in this study varied from 0.176 mm to 1.50 mm. The thickness of the epoxy was determined using Eq. (1):

$$t_{\text{epoxy}} = \frac{t_{\text{total}} - t_{\text{conc}} - 2t_{\text{frp}}}{2} \tag{1}$$

where t_{epoxy}, t_{conc} and t_{frp} are the total thickness of the (FRP, epoxy, concrete, epoxy and FRP) composite, the concrete thickness, and the FRP thickness (Fig. 1). The FRP thickness was 0.39 mm as reported by the CFRP manufacturer's datasheet. The total thickness and the concrete thickness were measured using a digital micrometer with 0.001 mm (1 μm) accuracy. The total thickness and the concrete thicknesses used in Eq. (1) represent the mean values determined from 40 measurements. Table 2 summarizes the shear stress levels and the epoxy layer thickness for testing specimens denoted S1, S2 and S3.

Fig. 2a schematically presents the test setup for the shear creep test. The concrete block was attached to a horizontal cantilever steel beam supported on a roller support by another steel frame fixed to the table. The test setup details can also be seen in Fig. 2b. The load was applied to the specimen by applying a weight to the other end of the cantilever as shown in Fig. 2a and b.

The deformation was monitored by observing the displacement of six fixed points at two faces on the specimens for up to 6 month time period. Fig. 1 shows the location of these fixed points denoted D1–D6. By observing the change in distance between these points, creep displacement can be computed as discussed below. In the present study, the distance between these fixed points was measured with 0.001 mm resolution. The distance between D1 and D3, and D5 and D6 were also measured to compensate for concrete shrinkage. Our experimental observations showed that shrinkage strains were insignificant due to the fact that the concrete specimens were left in the dry laboratory

Table 2
Properties of test specimens and test results (ultimate creep coefficient and retardation time)

Specimens		Shear stress/ultimate shear (%)	Epoxy thickness (mm)	Ultimate creep coefficient	Retardation time (days)
S1	Face 1	15	0.242	1.17	43.3
	Face 2			1.02	2.1
S2	Face 1	31	0.176	2.89	1.1
	Face 2			2.94	1.7
S3	Face 1	31	1.50	2.59	0.2
	Face 2			2.39	0.1

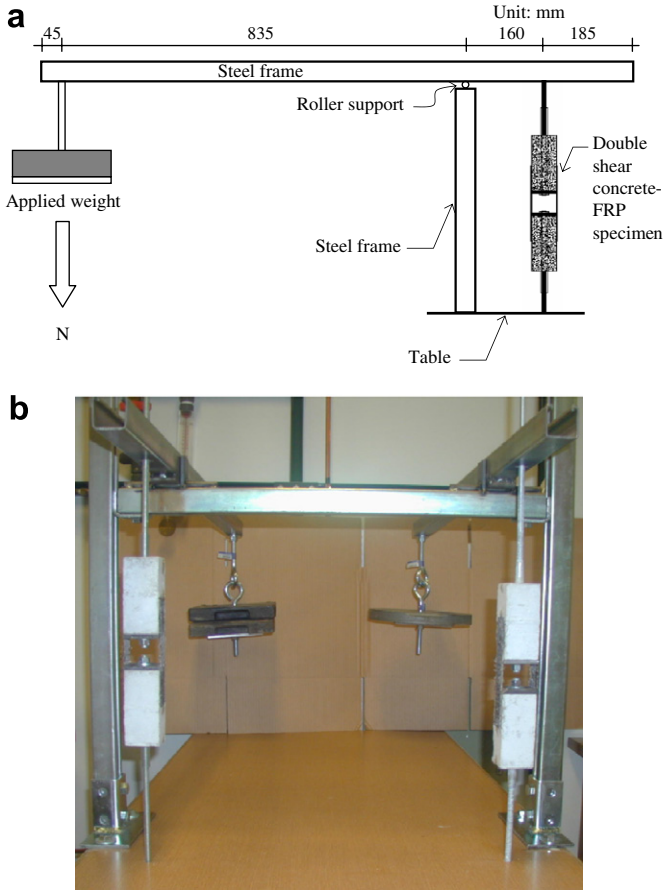

Fig. 2. Creep test setup.

environment long time before load application. Therefore, the creep deformation was evaluated by using the variation of distance between fixed points D1 and D6.

2.2. Modeling shear creep

For a given sustained stress $\sigma(t_0)$ applied at t_0, a specific creep $c_{sp}(t,t_0)$ evaluated at time t can be defined as

$$c_{sp}(t,t_0) = \frac{\varepsilon_{cr}(t,t_0)}{\sigma(t_0)} \tag{2}$$

where $\varepsilon_{cr}(t,t_0)$ is the creep strain at time t due to application of the stress $\sigma(t_0)$ at time t_0. The ratio between the specific creep (c_{sp}) and the specific elastic strain (e_{sp}) is equal to the ratio of the creep strain and the elastic strain (ε_e). Here, the specific elastic strain indicates elastic strain (ε_e) caused by a unit sustained stress: $e_{sp} = \varepsilon_e/\sigma$. This ratio between the time dependent creep strain and the instantaneous elastic strain is widely used in structural design and is known as the creep coefficient $\phi(t,t_0)$

$$\phi(t,t_0) = \frac{\varepsilon_{cr}(t,t_0)}{\varepsilon_e} = \frac{c_{sp}(t,t_0)}{e_{sp}} \tag{3}$$

Moreover, the creep compliance $J(t,t_0)$ can be defined as

$$J(t,t_0) = \frac{1}{E(t_0)} + c_{sp}(t,t_0) \tag{4}$$

While researchers prefer using creep compliance, $J(t,t_0)$, defined in Eq. (4) for its recognized physical meaning [17,18], we utilize the creep coefficient $\phi(t,t_0)$ to describe creep of epoxy due to its ease of use in the finite element model. Therefore, we limit our creep representation here to the creep coefficient $\phi(t,t_0)$.

For simplicity, the creep behavior of concrete was neglected because the compressive stress applied to the concrete block was significantly low compared with the compressive strength of concrete. Moreover, since CFRP has been reported to have very insignificant creep and stress relaxation [3,12,19], creep of the CFRP sheets was neglected. Therefore, the variation of distance between D1 and D6 according to time is attributed to shear creep of epoxy only. The creep strain $\gamma_{cr}(t)$ due to shear stresses can be defined as a function of the displacement between the fixed points D1 and D6 as shown schematically in Fig. 3 and as represented in Eq. (5):

$$\gamma_{cr}(t) = \frac{\Delta_{16}(t) - \Delta_{16}(t_0)}{2h} \tag{5}$$

where $\Delta_{16}(t)$ = total deformation (elastic plus creep) between the fixed points D1 and D6 at time t, $\Delta_{16}(t_0)$ = instantaneous elastic deformation between the fixed points D1 and D6, and h = thickness of epoxy layer. From Eq. (3), the shear creep coefficient $\phi(t,t_0)$ can be defined as

$$\phi(t,t_0) = \frac{\gamma_{cr}(t,t_0)}{\gamma_e} \tag{6}$$

where γ_e is instantaneous elastic shear strain of epoxy, which is defined as $\gamma_e = [\Delta_{16}(t_0) - \Delta_{16,FRP}(t_0)]/(2h)$. Substituting Eq. (5) into (6), the shear creep coefficient $\phi(t,t_0)$ can be evaluated from the experimental observations as

$$\phi(t,t_0) = \frac{\Delta_{16}(t) - \Delta_{16}(t_0)}{\Delta_{16}(t_0) - \Delta_{16,FRP}(t_0)} \tag{7}$$

According to Neville et al. [20], the creep behavior of viscoelastic materials can be well represented by a generalized exponential model as represented by Eq. (8):

$$\phi(t,t_0) = \phi_u(t_0)[1 - \exp(-t/\tau^*)] \tag{8}$$

where $\phi_u(t_0)$ = ultimate creep coefficient at infinite time, and τ^* = retardation time denoting the time when 63% of the creep has occurred. Many researchers used such expression in defining creep of viscoelastic materials [20]. In this study, the creep model parameters, $\phi_u(t_0)$ and τ^*, were determined using principles of curve fitting to minimize the root mean square error between the proposed model (Eq. (8)) and the experimental observation. It is worth noting that the creep model proposed in Eq. (8) might not be the best model to describe creep of epoxy at the concrete–FRP interfaces. However, this model has been chosen merely for its simple integration in the finite element analysis. Other creep models based on rheological analysis showed much enhanced ability to describe creep of epoxy

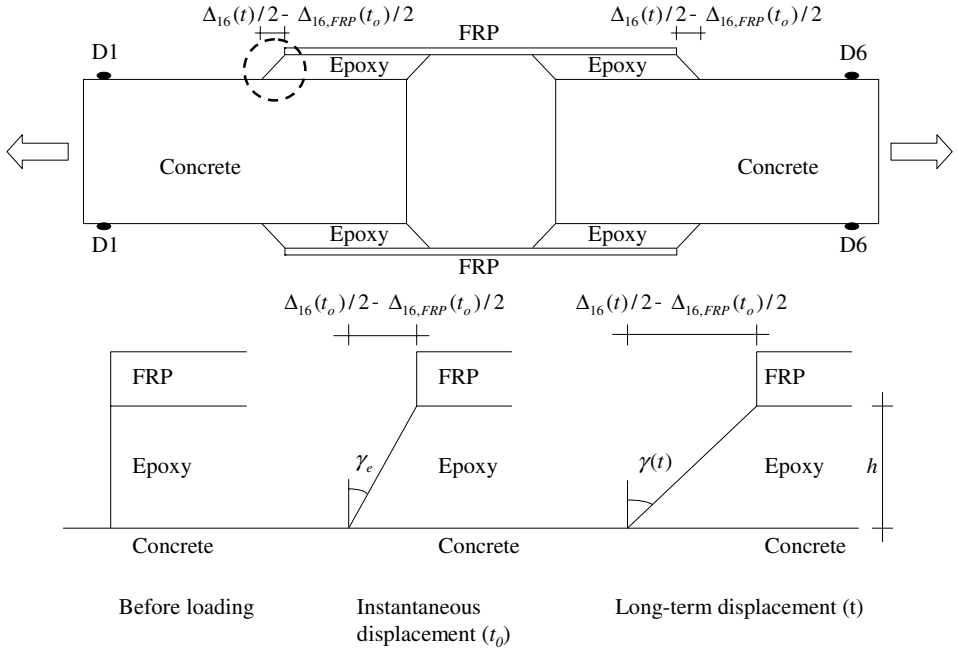

Fig. 3. The relationship between shear creep strain and measured displacement.

at the concrete–FRP interfaces compared with the above proposed model. These models are discussed elsewhere [16].

2.3. Finite element modeling

Time-dependent nonlinear finite element analyses using ANSYS® 7.11 [21] were performed to investigate the long-term behavior of concrete–FRP interfaces. The test setup was modeled using a 2D plane strain analysis. The choice of this type of model was governed by geometrical constraints such as the extremely thin epoxy layer. The epoxy was modeled using Plane 82 [21], a plane element with eight nodes allowing modeling of the creep behavior of epoxy. This element has two degrees of freedom for translations about the nodal x and y directions at each node. The time-dependent creep behavior of epoxy was modeled using the generalized exponential creep model suggested in Eq. (8). The creep model parameters, $\phi_u(t_0)$ and τ^*, obtained from test results were used in the finite element analysis. The CFRP sheet was modeled using Link 10 [21], a uniaxial tension element assuming elastic material behavior. Concrete was modeled by Plane 82 [21] assuming elastic material behavior considering the significantly low stresses in concrete compared with its tensile strength.

The finite element model of the double shear creep test specimen is shown in Fig. 4. Considering the symmetry of the test specimen, only a quarter of the specimen was modeled, and the boundary conditions of the FE model of the beams were adjusted to simulate symmetry conditions. To simulate the effect of the steel bearing plates, the translation of x direction was restraint. Fig. 4 also shows close view of the FE model of concrete–FRP interfaces. Two thousand and five hundred plane elements with

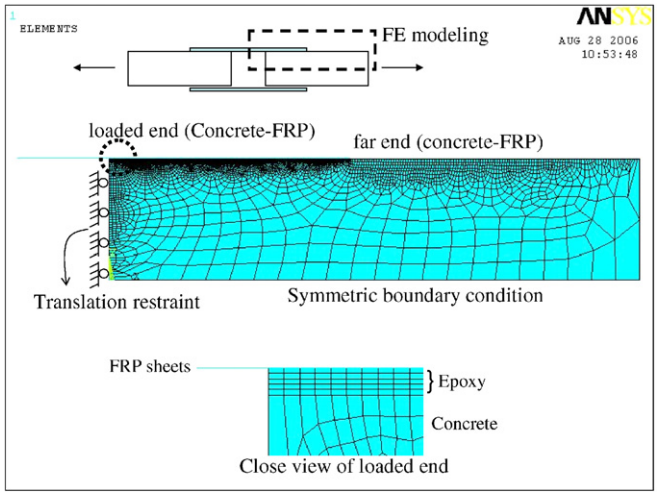

Fig. 4. Finite element model of double-shear test specimens.

five layers of plane elements were used to represent epoxy while 6007 plane elements with irregular polygon with eight nodes were used to represent concrete. The CFRP sheets were modeling using 516 line elements. Perfect bond at the interfaces concrete, epoxy, and FRP sheets was assumed. Considering the difference in widths between the CFRP/epoxy composite and the concrete specimens, elastic modulus of FRP sheets and epoxy were adjusted using the modification factor, β_w after Chen and Teng [14] to satisfy plane strain conditions.

$$\beta_w = \sqrt{\frac{2 - b_{frp}/b}{1 + b_{frp}/b}} \tag{9}$$

where b_{frp} and b are the widths of the FRP sheets and the concrete specimen. In the present study, β_w is calculated as

0.87 by using $b_{frp} = 35$ mm and $b = 50$ mm. Therefore, the adjusted elastic modulus of FRP sheets and epoxy were evaluated as $\beta_w E_F$ and $\beta_w E_E$, where E_F and E_E were the elastic modulus of FRP sheets and epoxy respectively.

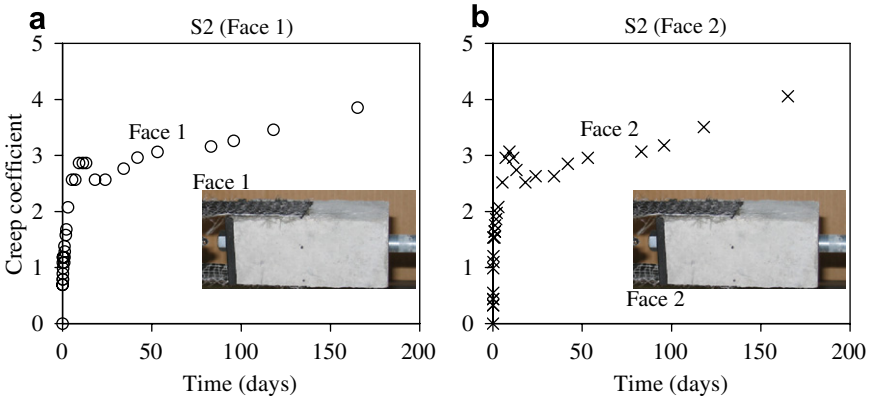

Fig. 5. Variation of creep coefficient of concrete–FRP interfaces obtained from creep shear test.

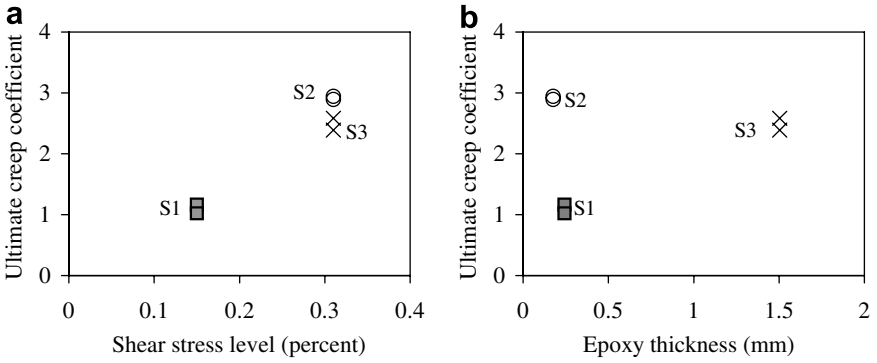

Fig. 6. Variation of ultimate creep coefficient of concrete–FRP interfaces.

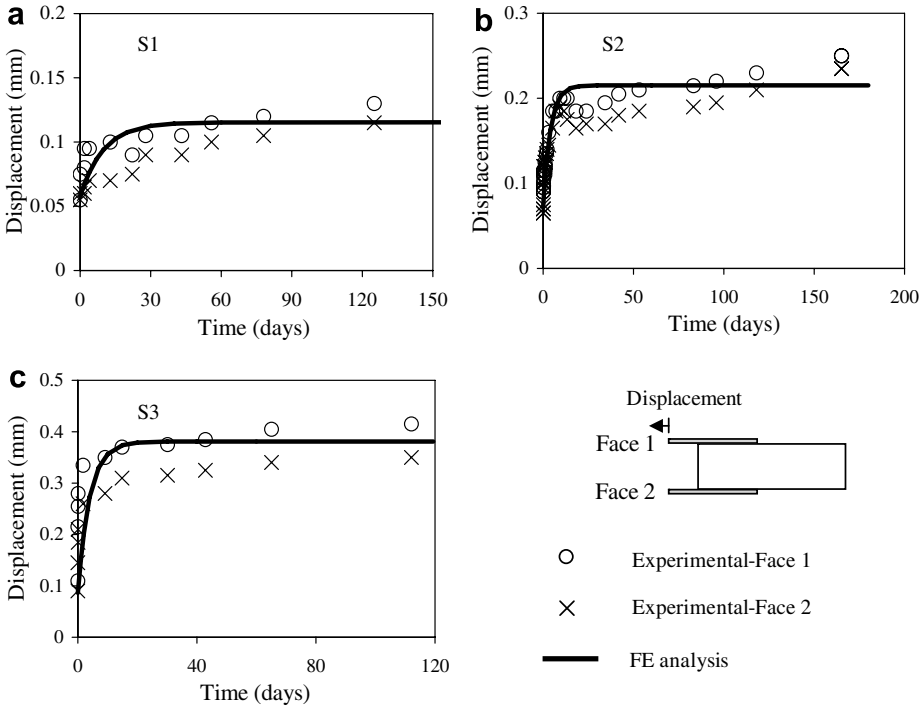

Fig. 7. Long-term displacement of test specimens obtained from test and FE analysis.

3. Results and discussion

The creep coefficient for the three specimens was evaluated using the method indicated above. Exemplar test results showing the change of the creep coefficient with time for specimen S2 are shown in Fig. 5. It can be observed that the ultimate creep coefficient was about 3.0 and creep retardation time τ^* ranged between 1 and 2 days. Recalling the fact typical retardation time of concrete ranges between 300 days and 900 days [20,22], it seems that creep of epoxy occurs within relatively short time period. The effect of significant difference in creep behavior between concrete and epoxy on the long-term behavior of concrete structures strengthened with FRP including stress redistribution requires further in-depth investigations.

Table 2 and Fig. 6 show the variation of the ultimate creep coefficient, $\phi_u(t_0)$, with the change of the shear stress level and the epoxy layer thickness for samples S1, S2, and S3. It can be observed from Fig. 6 that the ultimate creep coefficient, $\phi_u(t_0)$, was significantly increased with the increase of the shear stress level. The significance of the stress level on creep of different materials has been reported by other researcher [23,24]. On the other hand, the effect of the epoxy layer thickness on the ultimate creep coefficient $\phi_u(t_0)$ cannot be clearly inferred from the limited number of test results.

The long-term displacements predicted by the finite element analysis are presented in Fig. 7 and is compared with the displacements measured from the experiments. It can be observed that the FE modeling can accurately predict the long-term deformation of double shear test specimens and the displacement change with time due to creep. It is important to note that while both faces of the double shear specimens were created with the same materials and with the production accuracy to ensure identical behavior, in many occasions, the two faces showed a slight difference in their creep behavior. This fact can be observed in Fig. 7.

Fig. 8 shows the deformed shape of the specimens. As shown, the loaded and far ends show significant local deformations. These deformations showed to increase as time passes as a result of creep. Moreover, the principal tensile stress obtained from the FE analysis for specimen S2 is presented in Fig. 9. It can be observed that a significant stress concentration occurs at both loaded and far

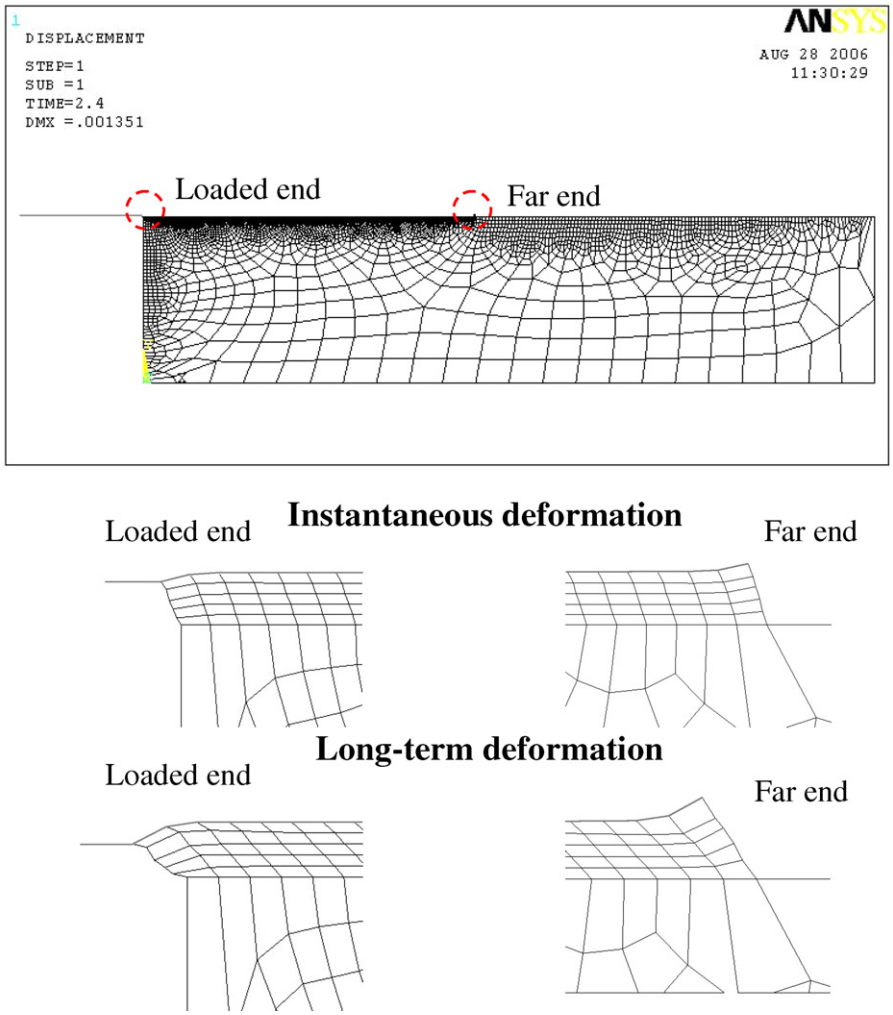

Fig. 8. Deformed shape of test specimens and close view of loaded end and far end.

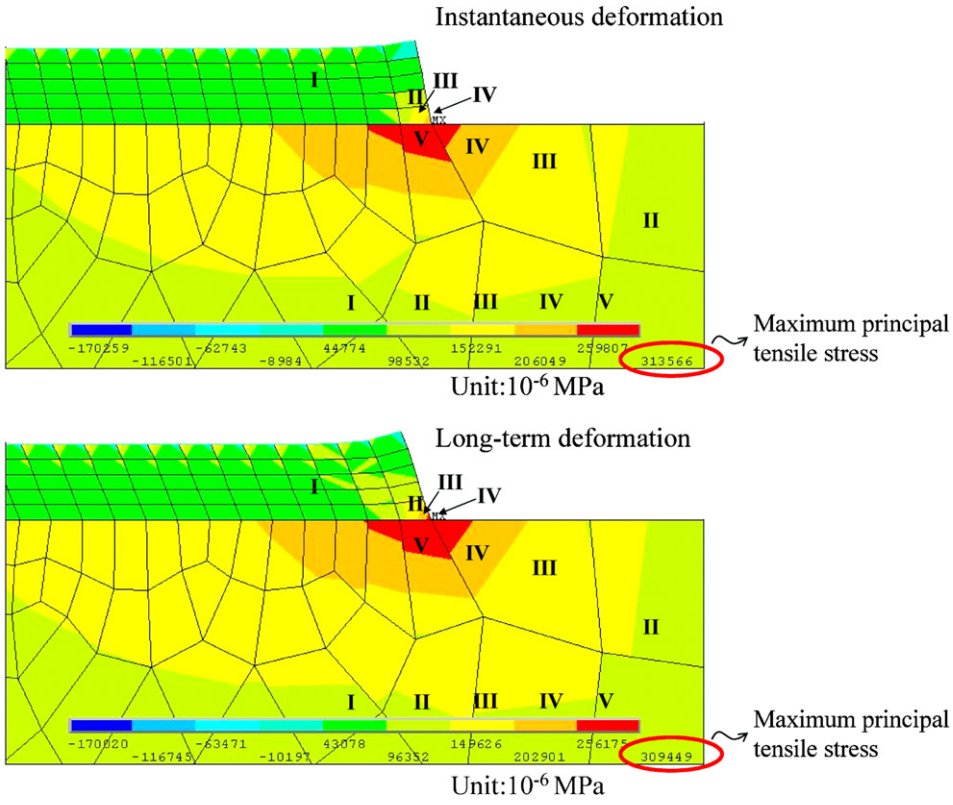

Fig. 9. Variation of principal tensile stress in specimens S2.

ends, and the principal tensile stress slightly decreases from 0.314 MPa to 0.309 MPa with time as a result of creep. Therefore, stress redistribution in concrete due to creep of epoxy at the interface might occur. The magnitude of this stress redistribution is dependent on many parameters including the shear stress level, the epoxy layer thickness as well as the concrete stiffness and creep criteria. If such redistributions occur in a reinforced concrete beam strengthened with FRP, stress relief at some locations might occur while stress increase at other locations causing tensile cracking might also occur. The experimental investigation and the proposed analytical creep model shed light on the complexity of the problem. The FE model shows the possible stimulation of stress redistribution in concrete elements strengthened with FRP due to creep of the epoxy at the concrete–FRP interfaces.

4. Conclusions

Creep shear experiments were performed to investigate the time-dependent behavior of epoxy at the concrete–FRP interfaces. The experimental investigation showed that the concrete–FRP interfaces yield significant time-dependent behavior. It is concluded that the shear stress to shear strength ratio is a primary factor affecting the long-term behavior of the concrete–FRP interfaces. Further experiments are underway to confirm theses findings.

A finite element model was developed to model the time-dependent behavior of the test specimen. The investigation showed that incorporating the time-dependent criteria of epoxy allowed the FE model to accurately predict the long-term deformation of the concrete–FRP composite. The FE analysis also showed that a limited stress redistribution in the concrete might occur as a result of shear creep of epoxy at the interface.

Acknowledgement

The financial support by the University of New Mexico is greatly appreciated.

References

[1] Lopez-Anido RA, Naik TR. Emerging materials for civil infrastructure: state of the art. ISBN 0-7844-0538-7. ASCE, 2000.
[2] Meier U. Strengthening of structures using carbon fibre/epoxy composites. Constr Build Mater 1995;9(6):341–51.
[3] Sayed-Ahmed EY, Shrive NG. A new steel anchorage system for post-tensioning applications using carbon fibre reinforced plastic tendons. Can J Civil Eng 1998;25:113–27.
[4] van Gemert D. Force transfer in epoxy-bonded steel–concrete joints. Int J Adhes Adhes 1980(1):67–72.
[5] Chajes MJ, Januszka TF, Mertz DR, Thomson Jr TA, Finch Jr WW. Shear strengthening of reinforced concrete beams using externally applied composite fabrics. ACI Struct J 1995;92(3):295–303.
[6] Yuan H, Wu ZS, Yoshizawa H. Theoretical solutions on interfacial stress transfer of externally bonded steel/composite laminates. J Struct Mech Earthquake Eng, JSCE 2001;675(1–55):27–39.
[7] Malek AM, Saadatmanesh H, Krishnamoorthy MR. Prediction of failure load of R/C beams strengthened with FRP plate due to stress concentration at the plate end. ACI Struct J 1998;95(2):142–52.

[8] Pecce M, Ceroni F. Modeling of tension-stiffening behavior of reinforced concrete ties strength with fiber reinforced plastic sheets. ASCE, J Comp Constr 2004;8(6):510–8.
[9] Niedermeier R. Stellungnahme zur Richtlinie für das Verkleben von Beton-bauteilen durch Ankleben von Stahllaschen-Entwurt März 1996. Schreiben Nr 1390 vom 30.10.1996 des Lehrstuhls für Massivbau, TU München, 1996.
[10] Hiroyuki Y, Wu Z. Analysis of debonding fracture properties of CFS strengthened member subject to tension. In: Proceedings of the third international symposium on non-metallic (FRP) reinforcement for concrete structures, Sapporo, Japan, 1997, p. 287–94.
[11] Teng JG, Chen JF, Smith ST, Lam L. FRP-strengthened RC structures. England: John Wiley & Sons, Ltd.; 2002, p. 245.
[12] ACI Committee 440.2R-02. Guide for the design and construction of externally bonded FRP systems for strengthening concrete structures, American Concrete Institute, Farmington Hills, MI, 2002.
[13] CEB-FIP Task group 9.3 FRP (fibre reinforced polymer) reinforcement for concrete structures. Externally bonded FRP reinforcement for RC structures, Technical report, Bulletin 14, 2001.
[14] Chen JF, Teng JG. Anchorage strength models for FRP and steel plates bonded to concrete. ASCE, J Struct Eng 2001;127(7):784–91.
[15] Chen JF, Teng JG. Shear capacity of FRP strengthened RC beams: FRP debonding. Constr Build Mater 2003;17(1):27–41.
[16] Meshgin P. Creep of epoxy at the concrete–fiber reinforced polymer (FRP) interfaces. MSc Thesis, Department of Civil Engineering, University of New Mexico, 2006.
[17] Nicholson LM, Gates TS. The influence of cross-link density on the creep compliance of an advanced polyimide. J Thermoplast Compos 2001;14(6):477–88.
[18] Romero N, Cárdenas S, Rivas H. Creep compliance-time behavior and stability of bitumen in water emulsions. J Rheol 2000;44(6): 1247–62.
[19] Yamaguchi T, Kato Y, Nishimura T, Uomoto T. Creep rupture of FRP rods made of aramid, carbon, and glass fibres. In: Proceedings of the third international symposium on non-metallic (FRP) reinforcement for concrete structures, Sapporo, Japan, 1997; vol. 2, p. 179–86.
[20] Neville A, Dilger W, Brooks JJ. Creep of plain and structural concrete. 1st ed. London, UK: Construction Press; 1983.
[21] SAS, ANSYS 7.1 Finite element analysis system, SAP IP, Inc. 2003.
[22] Bažant ZP. Creep of concrete. In: Buschow KHJ et al., editors. Encyclopedia of material: science and technology K.H.J, 2C. Amsterdam: Elsevier; 2001. p. 1797–800.
[23] Reda Taha MM, Noureldin A, El-Sheimy N, Shrive NG. Feedforward neural networks for modelling time-dependent creep deformations in masonry structures. In: Proceedings of the institution of civil engineers, structures in buildings 2004, vol. 157(Issue SB4), p. 279–92.
[24] Zhou Y, Fushitani B, Kubo T. Effect of stress level on bending creep behavior of wood during cyclic moisture changes. Wood Fiber Sci 2000;32(1):20–8.